

Multicriteria Design of Hybrid Power Generation Systems Based on a Modified Particle Swarm Optimization Algorithm

Lingfeng Wang and Chanan Singh, *Fellow, IEEE*

Abstract—Multisource hybrid power generation systems are a type of representative application of the renewables' technology. In this investigation, wind turbine generators, photovoltaic panels, and storage batteries are used to build hybrid generation systems that are optimal in terms of multiple criteria including cost, reliability, and emissions. Multicriteria design facilitates the decision maker to make more rational evaluations. In this study, an improved particle swarm optimization algorithm is developed to derive these nondominated solutions. Hybrid generation systems under different design scenarios are designed based on the proposed approach. First, a grid-linked hybrid system is designed without incorporating system uncertainties. Then, adequacy evaluation is conducted based on probabilistic methods by accounting for equipment failures, time-dependent sources of energy, and stochastic generation/load variations. In particular, due to the unpredictability of wind speed and solar insolation as well as the random load variation, time-series models are adopted to reflect their stochastic characteristics. An adequacy evaluation procedure including time-dependent sources, is adopted. Sensitivity studies are also carried out to examine the impacts of different system parameters on the overall design performance.

Index Terms—Adequacy evaluation, hybrid power generation system, multicriteria design, particle swarm optimization, probabilistic method, renewable energy, time-series models.

I. INTRODUCTION

WITH THE increasing concerns on air pollution and global warming, the clean green renewable sources of energy are expected to play more significant role in the global energy future [9], [12], [24]. Most of them are environmentally benign and do not contribute to the atmospheric pollution, acid rain, and global climate warming. Furthermore, due to public support and government incentives over recent decades, they are growing rapidly, not only in technical performance, but also in the breadth of applications. The public attention has remained focused on these renewable technologies as environmentally sustainable and convenient alternatives. Among them, wind power and solar power are the two most widely used renewable sources of energy since they feature certain

merits as compared with the conventional fossil-fuel-fired generation. For instance, wind turbine generators (WTGs) generate no pollution and they do not consume depleting fossil fuels. Photovoltaic (PV) systems produce no emissions, are durable, and demand minimal maintenance to operate. Unfortunately, these renewable sources of energy are essentially intermittent and quite variable in their output. Also, they require high capital costs. Thus, it is possible that power fluctuations will be incurred since both power sources are highly dependent on the weather conditions [8]. To mitigate or even cancel out the fluctuations, energy storage technologies, such as storage batteries (SBs) can be employed. SBs may absorb the surplus power and provide the deficit power in different operating situations [3], [4]. As a result, hybrid generation systems have attracted much attention [6], [7], [10], [13], [14], [18]. However, besides the fluctuations of time-dependent sources, there are various uncertainties existing in operations of such hybrid systems, e.g., possible equipment failures and stochastic generation/load variations. Therefore, reliability evaluation for the intended system using probabilistic methods is highly desired. In this investigation, adequacy evaluation theory is used in the design to ensure the system reliability in the presence of generating unit malfunctions. To reflect the stochastic characteristics of wind and solar power, an autoregressive moving average (ARMA) time series is used to model the wind speed and solar insolation at different time instants. Furthermore, the ARIMA time series is used to model the random variation of load demand. In this way, various uncertainties including equipment failures and random generation/load variations, are taken into account in the system design, which is expected to enhance system reliability in the face of different uncertainties.

In this paper, we employ a multicriteria approach to handle hybrid system design problems by taking into account multiple design objectives including economics, reliability, and pollutant emissions. Multicriteria design helps the decision maker reflect upon, articulate, and apply value judgments to determine reasonable tradeoffs thus leading to recommendations of corresponding alternatives [2], [21]. Thus, multicriteria design provides a viable way to reach tradeoffs among these design objectives with different preferences. Also, due to the high complexity and high nonlinearity of the design problem, a metaheuristics called particle swarm optimization (PSO) is adopted and improved accordingly in order to derive a set of nondominated solutions with sufficient diversity for decision-making support. PSO has turned out to be an outstanding optimizer due to its ability to

Manuscript received June 5, 2007; revised May 1, 2008. First published January 13, 2009; current version published February 19, 2009. This work was supported by the National Science Foundation under Grant ECS0406794: Exploring the future of distributed generation and microgrid networks. Paper no. TEC-00168-2007.

The authors are with the Department of Electrical and Computer Engineering, Texas A&M University, College Station, TX 77843 USA (e-mail: l.f.wang@ieee.org; singh@ece.tamu.edu).

Color versions of one or more of the figures in this paper are available online at <http://ieeexplore.ieee.org>.

Digital Object Identifier 10.1109/TEC.2008.2005280

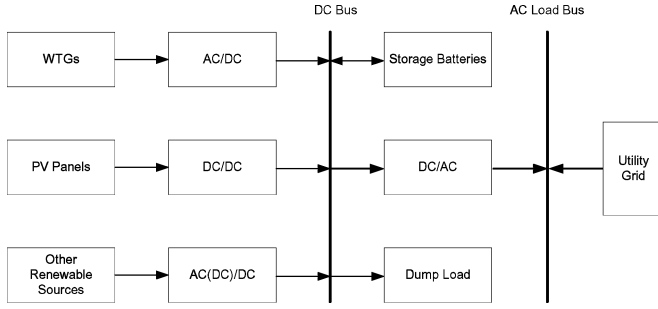


Fig. 1. Configuration of a typical hybrid generation system.

elegantly handle difficult optimization problems as well as its exceptional convergence performance.

The remainder of the paper is organized as follows. Section II formulates the hybrid system design problem including its multiple objectives coupled with a set of design constraints. Section III introduces the mechanism of PSO algorithms. The proposed multiobjective PSO (MOPSO) algorithm is detailed in Section IV. Simulation results and sensitivity studies for designing grid-linked hybrid systems without and with system uncertainties consideration are presented in Sections V and VI, respectively. Finally, conclusions are drawn and future research direction is suggested.

II. PROBLEM FORMULATION

As shown in Fig. 1, a typical hybrid generation system comprises different power sources including wind turbine generators, PV panels (PVs), and storage batteries (SBs). These power sources have different impacts on cost, environment, and reliability. In a hybrid generation system, they are integrated together and complement one another in order to serve the load while satisfying certain economic, environmental, and reliability criteria. The hybrid system can be operated autonomously or connected to the utility grid whose power is from the conventional fossil-fuel-fired generators (FFGs). Due to space restrictions, here only grid-linked system designs will be discussed. The multicriteria design of a stand-alone hybrid generation system can be referred to in [22].

The objective of this study is to achieve hybrid generation systems that should be appropriately designed in terms of economics, reliability, and environmental measures subject to physical and operational constraints/strategies. Two design scenarios are investigated, i.e., grid-linked hybrid generation systems without and with uncertainties consideration. Here, we start with the discussion of a hybrid system design without considering uncertainties. That is, neither generator failures nor stochastic generation/load variations is considered in the design. Some of the calculations formulated in this section are applicable to the hybrid system design incorporating adequacy evaluation including uncertainties discussed in Section VI.

A. Design Objectives

1) *Objective 1 (Costs)*: Cost estimation has been incorporated into the hybrid generation system design [6], [7]. The

total cost $COST$ (\$/year) includes initial cost, operational and maintenance (OM) cost for each type of power source, and the salvage value of each equipment which should be deducted

$$COST = \frac{\sum_{i=w,s,b} (I_i - S_{P_i} + OM_{P_i})}{N_p} + C_g \quad (1)$$

where w, s, b indicate the wind power, solar power, and battery storage, respectively; I_i, S_{P_i}, OM_{P_i} are the initial cost, present worth of salvage value, and present worth of operation and maintenance cost (OM) for equipment i , respectively; N_p (year) is the lifespan of the project; and C_g is the annual cost for purchasing power from the utility grid. Here, we assume that the lifetime of the project does not exceed those of both WTGs and PV arrays.

a) For the WTGs

$$I_w = \alpha_w A_w \quad (2)$$

where α_w (\$/m²) is the initial cost of WTGs; the present worth of the total salvage value is

$$S_{P_w} = S_w A_w \left(\frac{1 + \beta}{1 + \gamma} \right)^{N_p} \quad (3)$$

where S_w (\$/m²) is the salvage value of WTGs per square meter, β and γ are the inflation rate and interest rate, respectively; the present worth of the total OM in the project lifetime is

$$OM_{P_w} = \alpha_{OM_w} \times A_w \times \sum_{i=1}^{N_p} \left(\frac{1 + \nu}{1 + \gamma} \right)^i \quad (4)$$

where α_{OM_w} (\$/m²/year) is the yearly OM cost per unit area and ν is the escalation rate.

b) For the PV panels, the initial cost is

$$I_s = \alpha_s A_s \quad (5)$$

where α_s (\$/m²) is the initial cost; the present worth of the total salvage value is

$$S_{P_s} = S_s A_s \left(\frac{1 + \beta}{1 + \gamma} \right)^{N_p} \quad (6)$$

where S_s (\$/m²) is the salvage value of PVs per square meter of PV panels; the present worth of the total OM in the project lifetime is

$$OM_{P_s} = \alpha_{OM_s} \times A_s \times \sum_{i=1}^{N_p} \left(\frac{1 + \nu}{1 + \gamma} \right)^i \quad (7)$$

where α_{OM_s} (\$/m²/year) is the yearly OM cost per unit area and ν is the escalation rate.

c) For the storage batteries, since their lifespan is usually shorter than that of the project, the total present worth of capital investments can be calculated as follows:

$$I_b = \alpha_b \times P_{b_{cap}} \times \sum_{i=1}^{X_b} \left(\frac{1 + \nu}{1 + \beta} \right)^{(i-1)N_b} \quad (8)$$

where N_b is the lifespan of SBs, X_b is the number of times to purchase the batteries during the project lifespan N_p ,

the salvage value of SBs is ignored in this study, and the present worth of the total OM cost in the project lifetime is calculated as follows:

$$\text{OM}_{pb} = \alpha_{\text{OM}_b} \times P_{b_{\text{cap}}} \times \sum_{i=1}^{N_p} \left(\frac{1+\nu}{1+\gamma} \right)^i \quad (9)$$

where α_{OM_b} (\$/kWh/year) is the yearly OM cost per kilowatt-hour.

- d) For the grid-linked system design, the annual cost for purchasing power from the utility grid can be calculated as follows:

$$C_g = \sum_{t=1}^T P_{g,t} \times \varphi \quad (10)$$

where $P_{g,t}$ (\$/year) is the power purchased from the utility at hour t ; φ (\$/kWh) is the grid power price; and T (8760 h) is the operational duration under consideration.

2) *Objective 2 (Reliability)*: Reliability is used to assess the quality of load supply. Here, the energy index of reliability (EIR) is used to measure the reliability of each candidate hybrid system design. EIR can be calculated from expected energy not served (EENS) as follows:

$$\text{EIR} = 1 - \frac{\text{EENS}}{E} \quad (11)$$

where E is the yearly energy demand. The EENS(kWh/year) for the duration under consideration T (8760 h) can be calculated as follows:

$$\text{EENS} = \sum_{t=1}^T (P_{b_{\text{min}}} - P_{b_{\text{soc}}}(t) - P_{\text{sup}}(t)) \times U(t) \quad (12)$$

where $U(t)$ is a step function that is zero when the supply exceeds or equals to the demand, and equals one if there is insufficient power in period t ; $P_d(t)$ is the load demand during hour t , $P_{\text{sup}}(t) = P_{\text{total}}(t) - P_d(t)$ is the surplus power in hour t , $P_{\text{total}}(t)$ is the total power from WTGs, PVs, and FFGs during hour t

$$P_{\text{total}}(t) = P_w(t) + P_s(t) + P_g(t). \quad (13)$$

Here, $P_{b_{\text{soc}}}(t)$ is the battery charge level during hour t , and $P_{b_{\text{min}}}$ is the minimum permitted storage level, the term $P_{b_{\text{soc}}}(t) - P_{b_{\text{min}}}$ indicates the available power supply from batteries during hour t ; and provided that there is insufficient power in hour t

$$P_g(t) = \kappa \times (P_d(t) - P_w(t) - P_s(t) - P_b(t)) \quad (14)$$

where $\kappa \in [0, 1]$ indicates the portion of purchased power with respect to the hourly insufficient power; or else, $P_g(t) = 0$. Note that no equipment failures and unexpected load deviations are considered in calculating the EENS, which in this design is all contributed by the fluctuations of renewable power generation.

3) *Objective 3 (Pollutant Emissions)*: With the increasing concerns on environment protection, there are stricter regulations on pollutant emissions. The most important emissions considered in the power generation industry due to their highly damaging effects on the ecological environment are sulfur dioxide (SO_2) and nitrogen oxides (NO_x). These emissions can be

modeled through functions that associate emissions with power production for generating units. They are dependent on fuel consumption and take the quadratic form

$$\text{PE} = \alpha + \beta \times \sum_{t=1}^T P_{g,t} + \gamma \times \left(\sum_{t=1}^T P_{g,t} \right)^2 \quad (15)$$

where α , β , and γ are the coefficients approximating the generator emission characteristics.

B. Design Constraints

Due to the physical or operational limits of the target system, there is a set of constraints that should be satisfied throughout system operations for any feasible solution.

1) *Constraint 1 (Power Balance Constraint)*: For any period t , the total power supply from the hybrid generation system must supply the total demand P_d with a certain reliability criterion. This relation can be represented by

$$P_w(t) + P_s(t) + P_b(t) + P_g(t) \geq (1 - R)P_d(t) \quad (16)$$

$$P_w(t) + P_s(t) + P_b(t) + P_g(t) - P_{\text{dump}}(t) \leq P_d(t) \quad (17)$$

where P_w , P_s , P_b , P_g , $P_{\text{dump}}(t)$, and P_d are the wind power, solar power, charged/discharged battery power, power bought from grid, dumped power, and total load demand, respectively; R is the ratio of the maximum permissible unmet power with respect to the total load demand at each time instant. The transmission loss is not considered in this investigation.

The output P_{WTG} (kW/m²) from WTGs for wind speed V_t can be calculated as

$$P_{\text{WTG}} = \begin{cases} 0, & V_t < V_{ci} \\ a \times V_t^3 - b * P_r, & V_{ci} \leq V_t < V_r \\ P_r, & V_r \leq V_t \leq V_{co} \\ 0 & V_t > V_{co} \end{cases} \quad (18)$$

where $a = P_r / (V_r^3 - V_{ci}^3)$, $b = V_{ci}^3 / (V_r^3 - V_{ci}^3)$, P_r is the rated power, V_{ci} , V_r , and V_{co} are the cut-in, rated, and cut-out wind speed, respectively. The real electric power from WTGs can be calculated as follows:

$$P_w = P_{\text{WTG}} \times A_w \times \eta_w \quad (19)$$

where A_w is the total swept area of WTGs and η_w is their efficiency.

The output power P_s (kW) from PV panels can be calculated as follows:

$$P_s = H \times A_s \times \eta_s \quad (20)$$

where H (kW/m²) is the horizontal irradiance, A_s is the PV area, and η_s is the efficiency of the PV panels.

2) *Constraint 2 (Bounds of Design Variables)*: The swept area of WGTs should be within a certain range

$$A_{w_{\text{min}}} \leq A_w \leq A_{w_{\text{max}}} \quad (21)$$

Similarly, the area of PV arrays should also be within a certain range

$$A_{s_{\text{min}}} \leq A_s \leq A_{s_{\text{max}}} \quad (22)$$

The state of charge (SOC) of storage batteries $P_{b_{soc}}$ should not exceed the capacity of storage batteries $P_{b_{cap}}$ and should be larger than the minimum permissible storage level $P_{b_{min}}$, the total SB capacity should not exceed the allowed storage capacity $P_{b_{cap_{max}}}$, and the hourly charge or discharge power P_b should not exceed the hourly inverter capacity $P_{b_{max}}$. As a result

$$P_{b_{min}} \leq P_{b_{soc}} \leq P_{b_{cap}} \quad (23)$$

$$0 \leq P_{b_{cap}} \leq P_{b_{cap_{max}}} \quad (24)$$

$$P_b \leq P_{b_{max}}. \quad (25)$$

The amount of power bought from utility grid should be within a certain range

$$P_{g_{min}} \leq \sum_{t=1}^T P_{g,t} \leq P_{g_{max}} \quad (26)$$

where $P_{g_{min}}$ and $P_{g_{max}}$ are the minimum and maximum power allowed to be bought from the utility grid, respectively.

The coefficient κ indicates the portion of purchased power from utility grid with respect to the insufficient power

$$0 \leq \kappa \leq 1. \quad (27)$$

C. Problem Statement

In summary, for this grid-linked system design, the objective of optimum design for renewable hybrid generation system is to simultaneously minimize $COST(A_w, S_w, P_{b_{cap}}, \kappa)$ and $E(A_w, S_w, P_{b_{cap}}, \kappa)$, as well as maximize $EIR(A_w, S_w, P_{b_{cap}}, \kappa)$, subject to the constraints (16)–(27). The design parameters that should be derived include WTG-swept area $A_w (m^2)$, PV area $A_s (m^2)$, total battery capacity $P_{b_{cap}}$ (kWh), and the ratio of power purchased from grid κ .

D. Operation Strategies

The power outputs from WTGs and PVs have the highest priorities to feed the load. Only if the total power from wind and solar systems is insufficient to satisfy the load demand, the storage batteries can discharge a certain amount of energy to supply the load. If there is still not enough power to supply the load, a certain amount of power will be purchased from the utility grid. That is, the grid power has the lowest priority to feed the load. Furthermore, if there is any excess power from WTGs and PVs, the batteries will be charged to store a certain permissible amount of energy for future use. If there is surplus power from WTGs and PVs even after feeding the load and charging the SBs, the dump load will consume the spilled power.

III. MECHANISM OF PSO

PSO is a population-based stochastic optimization procedure inspired by certain social behaviors in bird groups and fish schools [15]. Assume x and v denote a particle position and its speed in the search space. Therefore, the i th particle can be represented as $x_i = [x_{i_1}, x_{i_2}, \dots, x_{i_d}, \dots, x_{i_M}]$ in the M -dimensional space. Each particle continuously records the best

solution it has achieved thus far during its flight. This fitness value of the solution is called pbest. The best previous position of the i th particle is memorized and represented as $pbest_i = [pbest_{i_1}, pbest_{i_2}, \dots, pbest_{i_d}, \dots, pbest_{i_M}]$. The global best gbest is also tracked by the optimizer, which is the best value achieved so far by any particle in the swarm. The best particle of all the particles in the swarm is denoted by gbest_d. The velocity for particle i is represented as $v_i = (v_{i_1}, v_{i_2}, \dots, v_{i_d}, \dots, v_{i_M})$. The velocity and position of each particle can be continuously adjusted based on the current velocity and the distance from pbest_{i_d} to gbest_d

$$v_{i_d}^{(t+1)} = \chi \times (w \times v_{i_d}^{(t)} + c_1 \times \text{rand}() \times (pbest_{i_d} - x_{i_d}^{(t)}) + c_2 \times \text{Rand}() \times (gbest_d - x_{i_d}^{(t)})) \quad (28)$$

$$x_{i_d}^{(t+1)} = x_{i_d}^{(t)} + v_{i_d}^{(t+1)}, \quad i = 1, 2, \dots, N, \quad d = 1, 2, \dots, M \quad (29)$$

where N is the number of particles in a swarm, M is the number of members in a particle, t is the counter of generations, $\chi \in [0, 1]$ is the constriction factor that controls the velocity magnitude, w is the inertia weight factor, c_1 and c_2 are acceleration constants, $\text{rand}()$ and $\text{Rand}()$ are uniform random values in a range $[0, 1]$, $v_i^{(t)}$ is the velocity of particle i in generation t , and $x_i^{(t)}$ is the current position of particle i in generation t .

IV. PROPOSED APPROACH

In this study, a constrained mixed-integer multiobjective PSO (CMIMOPSO) is developed to derive a set of nondominated solutions by appropriately combining different sources of energy subject to certain constraints. Different from the previous study [23], new schemes for diversity preservation of solutions are used in the proposed method.

A. Global Best Selection

In MOPSO, best plays an important role in directing the whole swarm in moving toward the Pareto front. Very often, the rapid swarm converging within the intermediate vicinity of gbest may lead to diversity loss and premature convergence. To resolve this, the fuzzy global best (f-gbest) scheme [17] is adopted in this study that is based on the concept of possibility measure to model the lack of information about the true optimality of gbest. In this scheme, gbest refers to the possibility of a particle at a certain location, rather than a sharp location as defined in traditional PSO algorithms. In this way, the particle velocity can be calculated as follows:

$$p_{c,d}^k = N(g_{g,d}^k, \delta) \quad (30)$$

$$\delta = f(k) \quad (31)$$

$$v_{i,d}^{k+1} = w \times v_{i,d}^k + c_1 \times r_1^k \times (p_{i,d}^k - x_{i,d}^k) + c_2 \times r_2^k \times (p_{c,d}^k - x_{i,d}^k) \quad (32)$$

where $p_{c,d}^k$ is the d th dimension of f-gbest in cycle k . The f-gbest is represented by a normal distribution $N(p_{g,d}^k, \delta)$, where

δ indicates the degree of uncertainty regarding the optimality of the gbest position. To reflect the reduction of this uncertainty as the search proceeds, δ can be defined as a nonincreasing function of the number of iterations. For instance, here $f(k)$ is defined as a simple function

$$f(k) = \begin{cases} \delta_{\max}, & \text{cycles} < \xi \times \text{max_cycles} \\ \delta_{\min}, & \text{otherwise} \end{cases} \quad (33)$$

where ξ is a user-specified parameter that affects the change of δ . We can see that the f-gbest function is designed to enable the particles to explore a region beyond that defined by the search trajectory of the original PSO. f-gbest encourages global exploration at the early search stage when δ is large, and facilitates local fine-tuning at the late stage when δ decreases. Thus, this scheme tends to reduce the possibility of premature convergence as well as enhance the population diversity.

B. Local Search

In this investigation, the combination of a local search termed synchronous particle local search (SPLS) [17] into MOPSO can be regarded as an effective measure for preserving distribution diversity and uniformity as well as speeding up the search process. SPLS carries out guided local fine-tuning so as to promote the distribution of nondominated solutions, whose computational procedure is laid out in the following [17]:

- 1) Choose S_{LS} individuals randomly from the population.
- 2) Choose N_{LS} nondominated individuals with the best niche count from the archive and store them in the selection pool.
- 3) Allocate an arbitrary nondominated individual from the selection pool to each of the S_{LS} individuals as gbest.
- 4) Allocate an arbitrary search space dimension for each of the S_{LS} individuals.
- 5) *Assimilation operation*: With the exception of the assigned dimension, update the position of S_{LS} individuals in the search space with the selected gbest position.
- 6) Update the position of all S_{LS} assimilated individuals using (30)–(32) along the preassigned dimension only.

C. Representation of Candidate Solutions

The design variables including WTG-swept area, PV area, amount of power purchased from the grid, and total SB capacity are encoded as the position value in each dimension of a particle. Several member positions indicate the coordinate of the particle in a multidimensional search space. Each particle is considered as a potential solution to the optimal design problem, since each of them represents a specific configuration of the hybrid generation system. Excluding $P_{b_{cap}}$, all the remaining positions are real-coded. The i th particle (i.e., candidate design) D_i can be represented as follows:

$$D_i = [P_{w,i}, P_{s,i}, P_{b_{cap},i}, \kappa_i], \quad i = 1, 2, \dots, N \quad (34)$$

where κ is ratio of power bought from the grid with respect to the deficit power, and the total SB capacity $P_{b_{cap}}$ is encoded using three binary bits.

D. Data Flow of the Optimization Procedure

The computational procedure of the proposed method is as follows:

- Step 1*: Specify the lower and upper bounds of WTG-swept area, area of PV panels, number of batteries, and other predetermined parameters.
- Step 2*: Randomly generate a population of particles. The speed and position of each particle are initialized.
- Step 3*: Evaluate each particle D_i in the population based on the concept of Pareto dominance.
- Step 4*: Store the nondominated solutions found so far in the archive.
- Step 5*: Initialize the memory of each particle where a single personal-best pbest is stored. The memory is contained in another archive.
- Step 6*: Increase the iteration number by one.
- Step 7*: Choose the personal-best position pbest for each particle based on the memory record; Choose the global best gbest according to the aforementioned f-gbest selection mechanism. Meanwhile, local search based on SPLS is carried out. The niching and fitness sharing mechanism is also applied throughout this process for enhancing the diversity of solutions.
- Step 8*: Update the member velocity v of each individual D_i . For the real-encoded design variables

$$\begin{aligned} v_{i_d}^{(t+1)} &= \chi \times (w \times v_i^{(t)} + c_1 \times \text{rand}()) \\ &\quad \times (\text{pbest}_{i_d} - P_{G_{i_d}}^{(t)}) + c_2 \times \text{Rand}() \\ &\quad \times (\text{gbest}_d - P_{G_{i_d}}^{(t)}), \quad i = 1, \dots, N; d = 1, 2. \end{aligned} \quad (35)$$

- Step 9*: Update the member position of each particle D_i based on (29). For real-coded variables

$$D_{i_d}^{(t+1)} = D_{i_d}^{(t)} + v_{i_d}^{(t+1)}. \quad (36)$$

For the binary-encoded design variable, update the member position based on the updating rule for discrete variables [16].

Following this, add the turbulence factor into the current position. For all the positions

$$D_{i_d}^{(t+1)} = D_{i_d}^{(t+1)} + R_T D_{i_d}^{(t+1)} \quad (37)$$

where R_T is the turbulence factor that is used to enhance the solution diversity by refraining the search from undesired premature convergence.

- Step 10*: Update the archive that stores nondominated solutions according to the Pareto-optimality-based selection criteria [23].
- Step 11*: If the current individual is dominated by the pbest in the memory, then keep the pbest in the memory; Otherwise, replace the pbest in the memory with the current individual.
- Step 12*: If the maximum number of iterations is reached, then go to Step 13; otherwise, go to Step 6.

TABLE I
DATA USED IN THE SIMULATION PROGRAM

System parameters	Values
Efficiency of WTG (η_w)	50%
Efficiency of PV (η_s)	16%
Efficiency of SB (η_b)	82%
Inflation rate (β)	9%
Interest rate (γ)	12%
Escalation rate (ν)	12%
Life span of project (N_p)	20 years
Life span of WTG (N_w)	20 years
Life span of PV (N_s)	22 years
Life span of SB (N_b)	10 years
PV panel price (α_s)	450\$/m ²
WTG price (α_w)	100\$/m ²
SB price (α_b)	100\$/KWh
PV panel salvage value (S_s)	45\$/m ²
WTG salvage value (S_w)	10\$/m ²
OM costs of WTG (α_{OM_w})	2.5\$/m ² /year
OM costs of PV panel (α_{OM_s})	4.3\$/m ² /year
OM costs of SB (α_{OM_b})	10\$/KWh
Cut-in wind speed (V_{ci})	2.5 m/s
Rated wind speed (V_r)	12.5 m/s
Cut-out wind speed (V_{co})	20.0 m/s
Rated WTG power (P_r)	4.0 kW
Period under observation (T)	8760 hours
Maximum swept area of WTGs ($A_{w_{max}}$)	10,000m ²
Minimum swept area of WTGs ($A_{w_{min}}$)	400m ²
Maximum area of PV panels ($A_{s_{max}}$)	200m ²
Minimum area of PV panels ($A_{s_{min}}$)	8,000m ²
Maximum conversion capacity ($P_{b_{max}}$)	3 kWh
Minimum storage level ($P_{b_{min}}$)	3 kWh
Rated battery capacity (P_{b_r})	8 kWh
Maximum total SB capacity ($P_{b_{max}}$)	40 kWh
Price of utility grid power (φ)	0.12\$/kWh

Step 13: Print out a set of Pareto-optimal solutions from the archive as the final possible system configuration.

V. CASE STUDY: SYSTEM DESIGN WITHOUT INCORPORATING UNCERTAINTIES

In this section, the tradeoff solutions are derived for a grid-linked hybrid system without incorporating system uncertainties, and some sensitivity studies are carried out.

A. System Parameters

The data used in the simulation program are listed in Table I [7]. The hourly wind speed patterns, the hourly insolation conditions, and the hourly load profile are shown in Fig. 2. These time-series data will be used by the ARMA model [5] to derive forecasted wind speed and solar insolation, which are then used to calculate the available wind power, solar power, and the insufficient or surplus power at each time instant.

B. PSO Parameters

In the simulations, both the population and archive sizes are set to 100, and the maximum number of iterations is set to 500. The acceleration constants c_1 and c_2 are both chosen as 1. Both turbulence factor and niche radius are set to 0.02. The inertia weight factor w decreases when the number of generations increases

$$w = w_{\max} - \frac{w_{\max} - w_{\min}}{\text{iter}_{\max}} \times \text{iter} \quad (38)$$

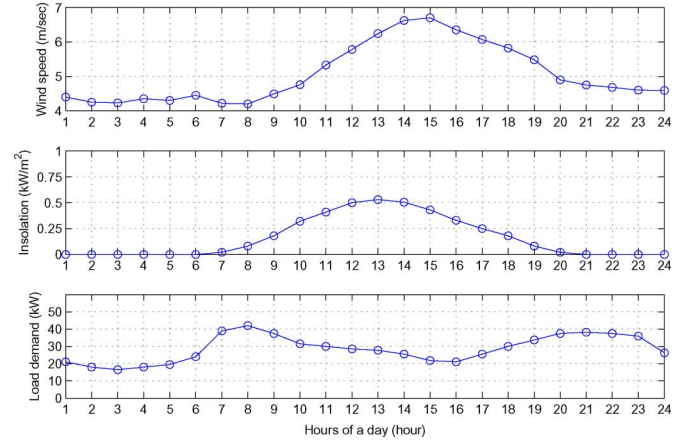


Fig. 2. Hourly mean wind speed, insolation, and load profiles.

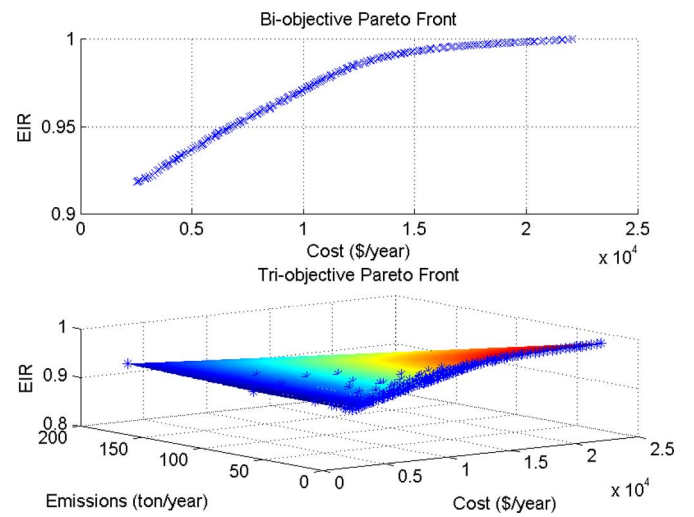


Fig. 3. Pareto fronts for bi- and triobjective optimization scenarios.

TABLE II
TWO ILLUSTRATIVE NONDOMINATED SOLUTIONS FOR TRIOBJECTIVE OPTIMIZATION

Variables/objectives	Design 1	Design 2
A_w (m ²)	810	680
A_s (m ²)	40	40
$P_{b_{cap}}$ (kWh)	16	16
κ	0.34	0.58
Cost (\$/year)	7,919.55	7,012.10
EIR	0.9579	0.9521
Emissions (ton/year)	17.0836	59.8295

where iter_{\max} is the maximum number of iterations and iter is the current number of iterations. This mechanism helps achieve the balance between exploration and exploitation in the search process. The simulation program is coded using C++ and executed in a 2.20-GHz Pentium-4 processor.

C. Simulation Results

The Pareto-optimal fronts evolved using the proposed approach for bi- and triobjective optimization problems are shown in Fig. 3, and two illustrative nondominated solutions are listed in Table II.

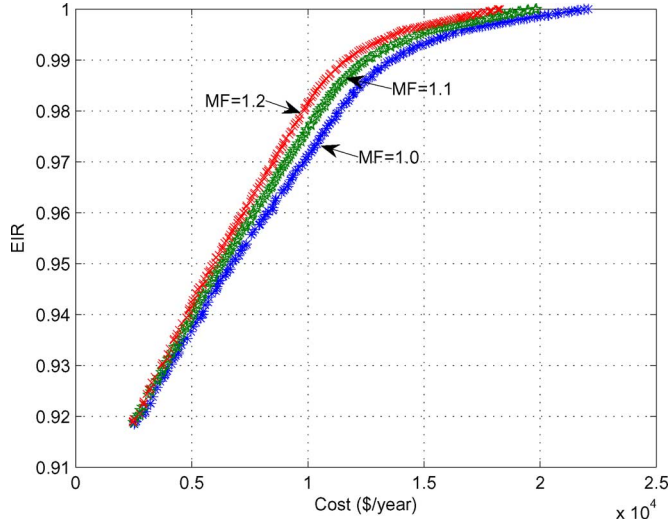


Fig. 4. Pareto fronts obtained from different mean wind speeds.

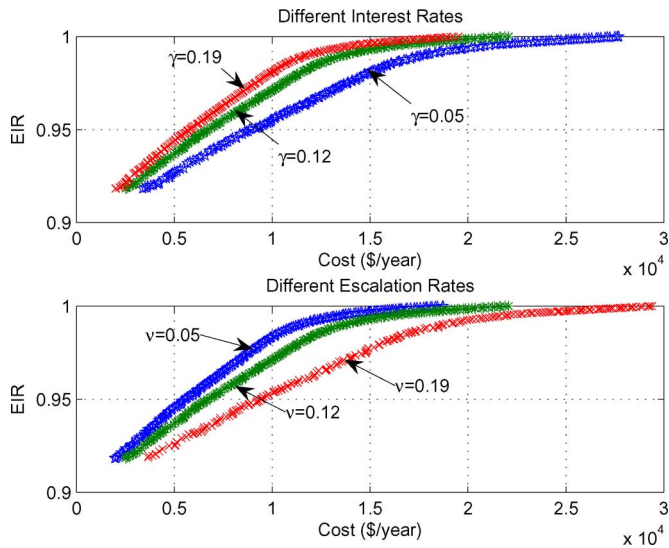


Fig. 5. Pareto fronts obtained from different economic rates.

D. Sensitivity to System Parameters

Here, the sensitivity analysis is carried out to examine the effects of changing the values of certain system parameters on the final derived nondominated solutions. For instance, the mean wind speeds are changed by different multiplication factors (MFs), and different economic rates are also examined. The results are illustrated in Figs. 4 and 5, respectively. From Fig. 4, we can appreciate the importance of site locations for a wind power plant. The simulation results shown in Fig. 5 fit with the cost estimation equations described in Section II.

VI. ADEQUACY-CONSTRAINED DESIGN INCORPORATING SYSTEM UNCERTAINTIES

In the previous section, a grid-linked hybrid system is designed without including uncertain factors. The design of an adequacy-constrained hybrid system using probabilistic methods is discussed in this section. Besides different problem

formulations, the focal points of these two design scenarios are also different in some sense. In the previous design, the generation system with WTGs, PVs, and SBs is treated as the base system. Only if there is insufficient power, a certain amount of power can be purchased from the utility grid. Conversely, in this design, the base system is the traditional utility grid and the renewable generation system is incorporated into it. The main intention here is to investigate the impact of different penetration levels of renewable energy on the overall system performance.

Probabilistic methods are now being used more widely in power system operations and planning due to a variety of uncertainties involved. For instance, adequacy evaluation is an important component to ensure proper operations of power systems in the presence of various uncertainties. Adequacy analysis of hybrid generating systems including time-dependent sources has been investigated in [11], [19], and [20]. Here, an efficient reliability evaluation technique proposed in [11] is used to calculate the reliability indices including expected unserved energy (EUE), loss of load expectation (LOLE), and loss of load frequency (LOLF), which are three fundamental indices for adequacy assessment of generating systems. The main idea of this method is to divide the generating system into a subsystem including all the conventional units and a set of subsystems each of which contains a possibly fluctuating unconventional source.

A. Calculation of Adequacy Indices

The load is represented as a chronological sequence of N_T discrete values P_{d_t} for successive time steps $t = 1, 2, \dots, N_T$. Each time step has equal duration $\Delta T = T/N_T$, where T is the entire period of observation. The general expressions for calculating the three indices are as follows:

$$EUE = \Delta T \sum_{t=1}^{N_T} U_t \quad (39)$$

where U_t is the unserved load during the time-step t and it can be calculated by

$$U_t = \sum_{X_t > X_{cco_t}} (X_t - X_{cco_t}) P(X_t) \quad (40)$$

where X_t is the total capacity outage at time instant t , $P(X_t)$ is the probability that a system capacity outage occurs exactly equal to X_t , and X_{cco_t} is the critical capacity outage at time instant t

$$X_{cco_t} = P_{g_t} + P_{w_t} + P_{s_t} - P_{d_t}. \quad (41)$$

In the aforesaid definition, the term $P_{g_t} + P_{w_t} + P_{s_t}$ indicates the effective total system capacity (that is, the summation of FFG power P_g , wind power P_w , and solar power P_s) at time instant t provided that all the units are available, and P_{d_t} is the load in period t . When $X_t > X_{cco_t}$, capacity deficiency occurs

$$LOLE = \frac{\Delta T}{T} \sum_{t=1}^{N_T} LOLP_t \quad (42)$$

where $LOLP_t$ is the loss of load probability during hour t

$$LOLF = \frac{\Delta T}{T} \sum_{t=1}^{N_T} (F_t^d + F_t^c + F_t^u) \quad (43)$$

where F_t^d is the frequency component caused by the load variation and fluctuation in the intermittent sources; and F_t^c and F_t^u are components of frequency due to interstate transitions in conventional and unconventional subsystems.

Distinguished from the negative margin and clustering methods, in this method the mean capacity outage table is constructed to simultaneously compute EUE, LOLE, and LOLF with reduced computational cost [11]. The computational procedure for these three indices is as follows:

- 1) Build the capacity outage table, the cumulative outage probability, and frequency tables for the conventional subsystem, using the unit addition algorithm.
- 2) Build the capacity outage table, the cumulative outage probability, and frequency tables for each unconventional subsystem considering the availability of intermittent sources, in a similar fashion.
- 3) Build the capacity outage table for the overall system through combining capacity outage tables constructed in the aforesaid two steps.
- 4) Build the mean capacity outage table for the conventional subsystem based on the recurrence approach.
- 5) Calculate the hourly contributions to the indices.
- 6) Calculate EUE, LOLE, and LOLF by summation over the whole period of observation.

B. Problem Formulation

In this design scenario, only WTGs and PVs are used. Thus, the total cost $COST(\$/\text{year})$ can be changed as follows:

$$COST = \frac{\sum_{i=w,s} (I_i - S_{P_i} + OM_{P_i})}{N_p} \quad (44)$$

Here, the cost of generating FFG power is excluded from the total cost calculation in order to examine the impact of wind and solar power penetration level on the overall system design in a more explicit fashion.

The real power balance constraint in this design scenario can be represented by

$$P_{w_t} + P_{s_t} + P_{g_t} \geq (1 - R)P_{d_t} \quad (45)$$

$$P_{w_t} + P_{s_t} + P_{g_t} - P_{\text{dump}_t} \leq P_{d_t} \quad (46)$$

Furthermore, due to the fluctuations of available wind and solar power coupled with possible generator failures, the loss of load may be caused. To ensure a certain degree of system reliability, the indices of LOLE and LOLF should also be fulfilled besides the maximization of EIR

$$LOLE \leq LOLE_{\text{max}} \quad (47)$$

where $LOLE_{\text{max}}$ is the maximum LOLE allowed. In a similar manner, LOLF should also be less than or equal to the maximum value $LOLF_{\text{max}}$

$$LOLF \leq LOLF_{\text{max}}. \quad (48)$$

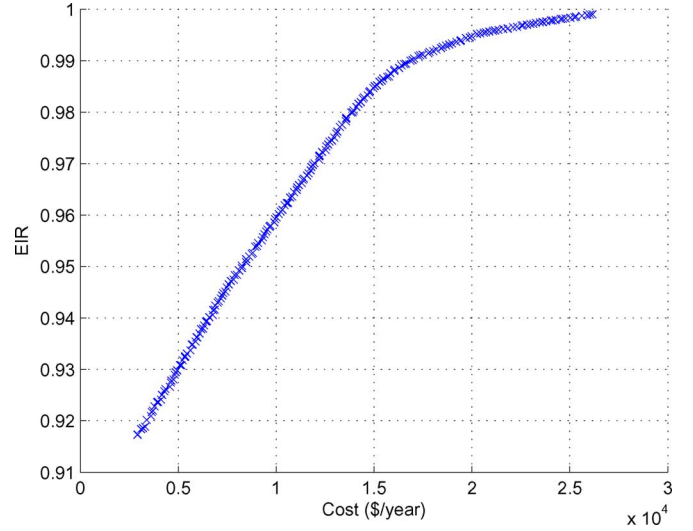


Fig. 6. Pareto front indicating a set of noninferior design solutions.

As can be seen in this study, one reliability index (EUE) is used as the design objective and the other two (LOLE and LOLF) are used as design constraints to ensure the generating system adequacy, which can be computed simultaneously.

In this scenario, the objective of optimum design for hybrid generating system with time-dependent sources is to simultaneously minimize $COST(A_w, A_s)$ as well as maximize $EIR(A_w, A_s)$, subject to the constraints (21)–(22) coupled with (45)–(48). The design parameters that should be derived include total WTG swept area A_w (m^2) and total PV area A_s (m^2).

C. Simulation Results

Three identical two-state FFGs are used together with multiple wind/solar generating units. Since solar power is much less prone to equipment failures, failures of PV cells are not considered in this investigation. In simulations, four identical WTGs are considered during the hybrid system design, and the capacity of each WTG is determined by the candidate solution under consideration. The rated FFG power (P_{FFG}) is 20 kW, and the reliability characteristics of each type of generating unit are as follows: FFG failure rate (λ_{FFG}) is 0.1 day^{-1} , FFG repair rate (μ_{FFG}) is 0.9 day^{-1} , WTG failure rate (λ_{WTG}) is 0.1 day^{-1} , and WTG repair rate (μ_{WTG}) is 0.4 day^{-1} . Furthermore, $LOLE_{\text{max}}$ and $LOLF_{\text{max}}$ are set 1.5 h/week and 1 occ./week, respectively.

The computational procedure used is basically the same as in the previous design, but some minor changes are needed to fit it into the current design scenario. For instance, the particle representation and design constraints should be modified accordingly. The Pareto-optimal front evolved in this design scenario using the proposed approach is shown in Fig. 6. The decision maker can choose a design solution from the derived set of noninferior solutions based on the specific design requirement or preference. Two illustrative nondominated solutions are listed in Table III. We can appreciate that the improvement of one objective is at the expense of deterioration of another objective. Thus, for any

TABLE III
TWO ILLUSTRATIVE SYSTEM CONFIGURATIONS FOR ADEQUACY-CONSTRAINED DESIGN

Variables	Design 1	Design 2
$A_w(m^2)$	880	1020
$A_s(m^2)$	40	160
Cost (\$/year)	7191.5	11233
EIR	0.9451	0.9653

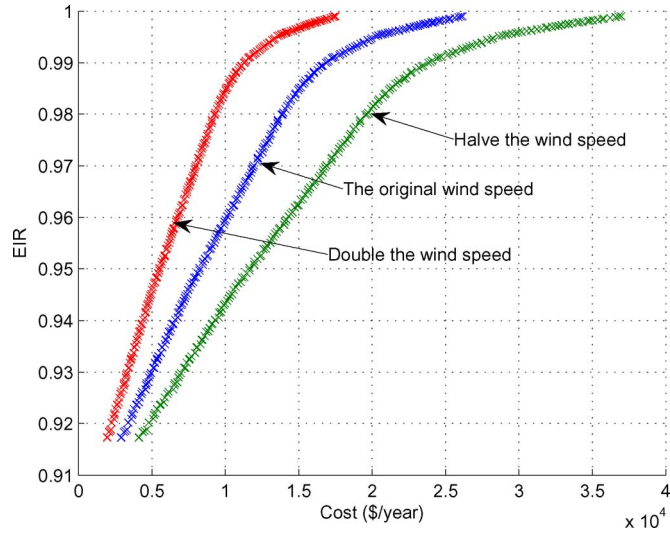


Fig. 7. Impacts of different wind speeds on derived Pareto fronts.

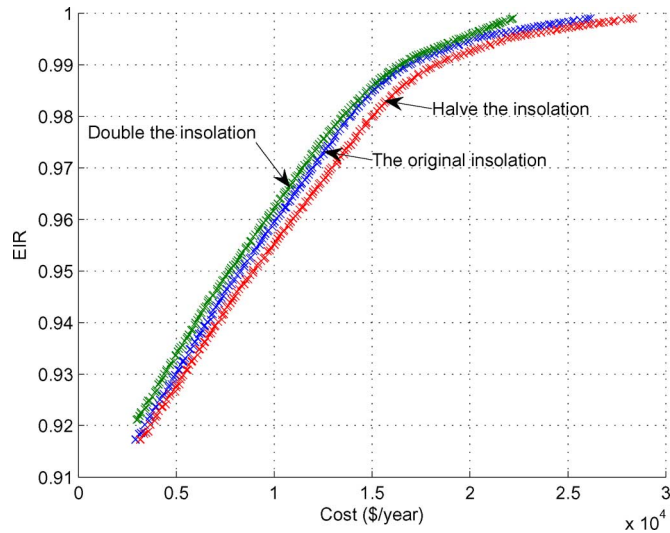


Fig. 8. Impacts of different insulations on derived Pareto fronts.

specific system design, a tradeoff between these two objectives should be reasonably made.

To examine the impacts of different wind speeds and insulations on the derived Pareto-optimal solutions, sensitivity studies are carried out. Figs. 7 and 8 show the tradeoff surfaces obtained in different scenarios in terms of wind speeds and solar insulations, respectively. Note that during the simulations, when different wind speeds are examined, the original insolation value is used. Likewise, when different insulations are examined, the original wind speed value is used. We can appreciate that at

TABLE IV
TWO ILLUSTRATIVE SYSTEM CONFIGURATIONS FOR ADEQUACY-CONSTRAINED DESIGN WITH LOAD FORECASTING

Variables	Design 1	Design 2
$A_w(m^2)$	880	1020
$A_s(m^2)$	40	160
Cost (\$/year)	7312	11418
EIR	0.9451	0.9653

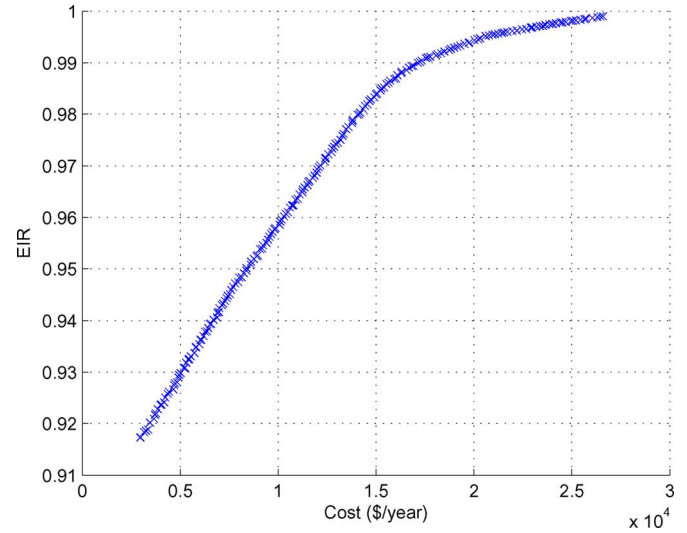


Fig. 9. Paretofront indicating a set of noninferior design solutions.

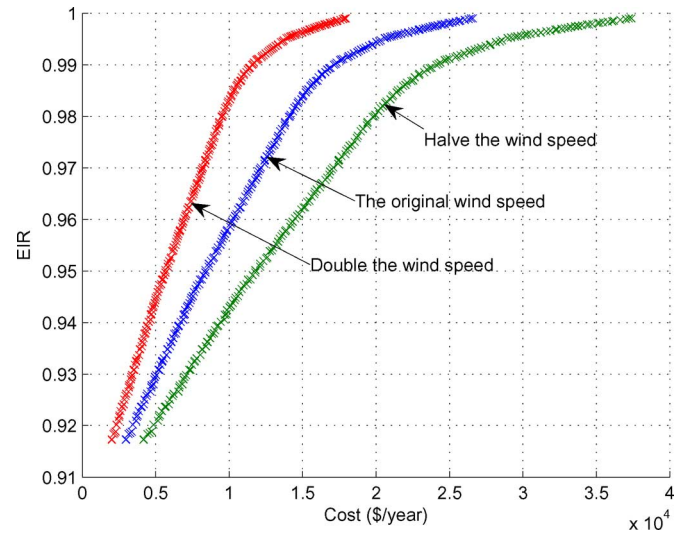


Fig. 10. Impacts of different wind speeds on Pareto fronts derived.

the same reliability level, the generating systems with the highest speed and insolation result in the lowest costs as compared to scenarios with lower wind speed and insolation. Thus, this confirms the previous observation that it is crucial to properly select power plant location when renewable sources of energy are involved. Usually, plant sites with richer renewable sources of energy can cause lower generation costs.

Next, the stochastic nature of load is considered, which is modeled through a time-series method called ARIMA [1]. Two illustrative nondominated solutions are listed in Table IV, and

Fig. 9 shows the tradeoff surface in this design scenario. We can appreciate that the stochastic characteristic of load demand induces somewhat more costs for ensuring the same reliability level. This is understandable since random variations of load may compromise the system reliability. Also, Fig. 10 shows the impacts of different wind speeds on the derived Pareto-optimal solutions. It further verifies the previous observation on the plant site selection.

VII. CONCLUDING REMARK

Distributed generation using sustainable clean green power promises to considerably restructure the energy industry that is evolving from fossil fuels toward renewables [9]. Meanwhile, there are many open-ended problems in this field awaiting to be resolved. In this paper, a hybrid power generation system including wind power and solar power is designed on the basis of cost, reliability, and emission criteria. A set of tradeoff solutions is obtained using the multicriteria metaheuristic method that offers many design alternatives to the decision maker. Moreover, in one of the designs, system uncertainties, such as equipment failures and stochastic generation/load variations, are considered by conducting adequacy evaluation based on probabilistic methods. In particular, the stochastic generation/load variations are modeled through time-series methods. Numerical simulations are used to illustrate the applicability and validity of the proposed MOPSO-based optimization procedure, and some sensitivity studies are also carried out. In future studies, other more complicated design scenarios may be incorporated into system designs.

REFERENCES

- [1] H. K. Alfares and M. Nazeeruddin, "Electric load forecasting: Literature survey and classification of methods," *Int. J. Syst. Sci.*, vol. 33, no. 1, pp. 23–34, 2002.
- [2] B. A. Akash, R. Mamlook, and M. S. Mohsen, "Multi-criteria selection of electric power plants using analytical hierarchy process," *Electr. Power Syst. Res.*, vol. 52, pp. 29–35, 1999.
- [3] J. P. Barton and D. G. Infield, "Energy storage and its use with intermittent renewable energy," *IEEE Trans. Energy Convers.*, vol. 19, no. 2, pp. 441–448, Jun. 2004.
- [4] G. N. Bathurst and G. Strbac, "Value of combining energy storage and wind in short-term energy and balancing markets," *Electr. Power Syst. Res.*, vol. 67, pp. 1–8, 2003.
- [5] G. E. P. Box and G. M. Jenkins, *Time Series Analysis: Forecasting and Control*. San Francisco, CA: Holden Day, 1976.
- [6] R. Chedid, H. Akiki, and S. Rahman, "A decision support technique for the design of hybrid solar-wind power systems," *IEEE Trans. Energy Convers.*, vol. 13, no. 1, pp. 76–83, Mar. 1998.
- [7] R. Chedid and S. Rahman, "Unit sizing and control of hybrid wind-solar power systems," *IEEE Trans. Energy Convers.*, vol. 12, no. 1, pp. 79–85, Mar. 1997.
- [8] E. A. DeMeo, W. Grant, M. R. Milligan, and M. J. Schuenger, "Wind plant integration: Costs, status, and issues," *IEEE Power Energy Mag.*, vol. 3, no. 6, pp. 38–46, Nov./Dec. 2005.
- [9] W. El Khattam and M. M. A. Salama, "Distributed generation technologies, definitions, and benefits," *Electr. Power Syst. Res.*, vol. 71, pp. 119–128, 2004.
- [10] M. A. El Sayes, M. G. Osman, and S. S. Kaddah, "Assessment of the economic penetration levels of photovoltaic panels, wind turbine generators and storage batteries," *Electr. Power Syst. Res.*, vol. 27, pp. 233–246, 1993.
- [11] S. Fockens, A. J. M. van Wijk, W. C. Turkenburg, and C. Singh, "Reliability analysis of generating systems including intermittent sources," *Int. J. Electr. Power Energy Syst.*, vol. 14, no. 1, pp. 2–8, 1992.
- [12] N. Jenkins, R. Allan, P. Crossley, D. Kirschen, and G. Strbac, *Embedded Generation*. (IEE Power and Energy Series 31). London, U.K.: The Institution of Electrical Engineers, 2000.
- [13] W. Kellogg, M. H. Nehrir, G. Venkataramanan, and V. Gerez, "Optimal unit sizing for a hybrid wind/photovoltaic generating system," *Electr. Power Syst. Res.*, vol. 39, pp. 35–38, 1996.
- [14] W. Kellogg, M. H. Nehrir, G. Venkataramanan, and V. Gerez, "Generation unit sizing and cost analysis for stand-alone wind, photovoltaic, and hybrid wind/PV systems," *IEEE Trans. Energy Convers.*, vol. 13, no. 1, pp. 70–75, Mar. 1998.
- [15] J. Kennedy and R. Eberhart, "Particle swarm optimization," in *Proc. IEEE Proc. Int. Conf. Neural Netw.*, Perth, Australia, 1995, pp. 1942–1948.
- [16] J. Kennedy and R. Eberhart, "A discrete binary version of the particle swarm optimization," in *Proc. IEEE Int. Conf. Syst., Man, Cybern.*, Orlando, FL, 1997, pp. 4104–4108.
- [17] D. S. Liu, K. C. Tan, C. K. Goh, and W. K. Ho, "A multiobjective memetic algorithm based on particle swarm optimization," *IEEE Trans. Syst., Man, Cybern. B. Cybern.*, vol. 37, no. 1, pp. 42–50, Feb. 2007.
- [18] T. Senjyu, D. Hayashi, N. Urasaki, and T. Funabashi, "Optimum configuration for renewable generating systems in residence using genetic algorithm," *IEEE Trans. Energy Convers.*, vol. 21, no. 2, pp. 459–466, Jun. 2006.
- [19] C. Singh and Y. Kim, "An efficient technique for reliability analysis of power systems including time dependent sources," *IEEE Trans. Power Syst.*, vol. 3, no. 3, pp. 1090–1094, Aug. 1988.
- [20] C. Singh and A. Lago Gonzalez, "Reliability modeling of generation systems including unconventional energy sources," *IEEE Trans. Power App. Syst.*, vol. PAS-104, no. 5, pp. 1049–1056, May. 1985.
- [21] T. J. Stewart, "A critical survey on the status of multiple criteria decision making theory and practice," *OMEGA Int. J. Manage. Sci.*, vol. 20, no. 5/6, pp. 569–586, 1992.
- [22] L. F. Wang and C. Singh, "Compromise between cost and reliability in optimum design of an autonomous hybrid power system using mixed-integer PSO algorithm," in *Proc. IEEE Int. Conf. Clean Elect. Power (ICCEP 2007)*, Capri, Italy, May, pp. 682–689.
- [23] L. F. Wang and C. Singh, "Environmental/economic power dispatch using a fuzzified multiobjective particle swarm optimization algorithm," *Electr. Power Syst. Res.*, vol. 77, no. 12, pp. 1654–1664, 2007.
- [24] H. L. Willis and W. G. Scott, *Distributed Power Generation: Planning and Evaluation*. New York: Marcel Dekker, 2000.



Lingfeng Wang received the B.Eng. degree from Zhejiang University, Zhejiang, China, the M.Eng. degree from the National University of Singapore, Singapore, and the Ph.D. degree in electrical and computer engineering from Texas A&M University, College Station.

He is currently with the Department of Electrical and Computer Engineering, Texas A&M University, College Station. His current research interests include renewable energy integration, electric power and energy systems, power system reliability, and computational intelligence.

tional intelligence.

Mr. Wang is the recipient of the Walter J. Karplus Summer Research Grant from the IEEE Computational Intelligence Society.



Chanan Singh (S'71–M'72–SM'79–F'91) received the B.S. (honors) degree from Punjab Engineering College, Chandigarh, India, and the M.S. and Ph.D. degrees from the University of Saskatchewan, Saskatchewan, Canada, all in electrical engineering.

He is currently is a Regents Professor and the Irma Runyon Chair Professor of electrical and computer engineering at Texas A&M University, College Station. From 1995 to 1996, he was the Director of the National Science Foundation (NSF) Power System Program. His current research interests include

electric power systems, theory and applications of system reliability, production costing, and power quality.

Prof. Singh is a Senior Texas Engineering Experiment Station (TEES) Fellow at Texas A&M University. He was the recipient of the IEEE 1998 Distinguished Power Engineering Educator Award and the 2008 Probabilistic Methods Applied to Power Systems (PMAPS) Merit Award from the PMAPS International Society.